



UDC 547.724

## ADSORPTION OF Co, Ni, Cu, Zn METAL IONS ON FULLERENE C<sub>60</sub> AND ON SINGLE-WALL CARBON NANOTUBES C<sub>48</sub> AS A DRIVEN FORCE OF COMPOSITE COATINGS' ELECTRODEPOSITION

Valentina V. Tytarenko,<sup>1</sup> Eduard Ph. Shtapenko,<sup>1</sup> Eugene O. Voronkov,<sup>1</sup> Aruna Vangara,<sup>2</sup>  
Vladimir A. Zabudovsky,<sup>1</sup> Wojciech Kolodziejczyk,<sup>3</sup> Karina Kapusta,<sup>3\*</sup> Sergiy I. Okovytyy<sup>4</sup>

<sup>1</sup>Dnipro National University of Railway Transport named after Academician V. Lazaryan, Lazaryana St, 2, Dnipro, 49010, Ukraine

<sup>2</sup>Rust College, 150 Rust Ave, Holly Springs, MS, 38635, USA

<sup>3</sup>Jackson State University, 1400 J. R. Lynch St, Jackson, MS, 39217, USA

<sup>4</sup>Dnipro National University, Haharina Ave, 72, Dnipro, 49000, Ukraine

Received 5 March 2021; accepted 31 March 2021; available online 30 April 2021

### Abstract

Composite electrodeposited films fabricated from aqueous solution of electrolytes that contain ions of metals along with carbon nanomaterial particles such as fullerene C<sub>60</sub> were investigated. Results for the cathodic polarization curve showed an increase in charge-transfer resistance. Phase composition analysis for metal films revealed the presence of carbon nanoparticles (CNPs) inside the metal matrix and significant changes in the crystal lattice. As it shown on microphotographies, addition of CNPs changes columnar growth patterns of metallic films to microlayered structure due to passivation of the surface.

Density Functional Theory was used for calculation of thermochemical, electronic and structural properties of metal ions complexes with CNPs. Calculated binding energies of the CNP-s-Me<sup>2+</sup> complexes suggests that an adsorption of Co<sup>2+</sup>, Ni<sup>2+</sup>, Cu<sup>2+</sup>, and Zn<sup>2+</sup> ions on the surface of fullerene C<sub>60</sub> and SWNT C<sub>48</sub> is possible and thermodynamically favorable. Binding affinity was found to be significantly stronger when the metal ion was adsorbed onto a surface of SWNT C<sub>48</sub>, than adsorption to the fullerene C<sub>60</sub>. With Cu<sup>2+</sup> complexes being the most thermodynamically stable, binding affinities were increasing in a row Co<sup>2+</sup><Zn<sup>2+</sup><Ni<sup>2+</sup><Cu<sup>2+</sup>. Calculated free binding energies showed a good correlation with the band gap, distances between metal ion and a surface of CNPs, dipole moments, delocalization of natural bond orbital (NBO) charges, and second ionization potential of metal ions.

Keywords: *Electrodeposition; Composite materials; Transition metals; Carbon nanoparticles; DFT.*

## АДСОРБЦІЯ ІОНОВ МЕТАЛІВ Co, Ni, Cu, Zn НА ФУЛЕРЕНІ C<sub>60</sub> І НА ОДНОСТІННІЙ ВУГЛЕЦЕВІЙ НАНОТРУБЦІ C<sub>48</sub> ЯК ДІЮЧА СИЛА ЕЛЕКТРООСАДЖЕННЯ КОМПОЗИЦІЙНИХ ПОКРИТТІВ

Валентина В. Титаренко<sup>1</sup>, Едуард П. Штапенко<sup>1</sup>, Євген О. Воронков<sup>1</sup>, Аруна Вангара<sup>2</sup>,  
Володимир О. Забудовський<sup>1</sup>, Войцех Колоджейчик<sup>3</sup>, Карина Капуста<sup>3</sup>, Сергій І. Оковитий<sup>4</sup>

<sup>1</sup>Дніпровський національний університет залізничного транспорту імені академіка В. Лазаряна, м Дніпро, 49010, Україна

<sup>2</sup>Раст-коледж, Холлі-Спрінгс, штат Массачусетс, 38635, США

<sup>3</sup>Междисциплинарний центр нанотоксичності, Кафедра хімії, фізики та атмосферних наук, Державний університет Джексона, Джексон, штат Массачусетс, 39217, США

<sup>4</sup>Дніпровський національний університет ім. Олесь Гончара, Дніпро, 49010, Україна

### Анотація

Досліджено композиційні плівки, осаджені у водних розчинах електролітів, що містять іони металів і частинки вуглецевих наноматеріалів, таких як фулерен C<sub>60</sub>. Результати дослідження катодних поляризаційних кривих показали збільшення опору переносу заряду. Аналіз фазового складу металевих плівок показав наявність вуглецевих наночастинок (ВНЧ) всередині металевій матриці і значні зміни у кристалічній решітці. З результатів дослідження мікрофотографій слідує, що додавання ВНЧ змінює структуру росту металевих плівок від стовбчатої до мікрошаруватої через пасивацію поверхні. У даній роботі теорія функціонала густини (ТФГ) була використана для розрахунку термодинамічних, електронних і структурних властивостей комплексів іонів металів з ВНЧ. Результати розрахунків енергії зв'язку комплексів ВНЧ- Me<sup>2+</sup> дозволяють припустити, що адсорбція іонів Co<sup>2+</sup>, Ni<sup>2+</sup>, Cu<sup>2+</sup> та Zn<sup>2+</sup> на поверхні фулерену C<sub>60</sub> і одностінної вуглецевої нанотрубки (ОВНТ) C<sub>48</sub> можлива і термодинамічно вигідна.

\*Corresponding author: [karina.kapusta@icnanotox.org](mailto:karina.kapusta@icnanotox.org)

© 2021 Oles Honchar Dnipro National University

doi: 10.15421/082108

Було виявлено, що енергія зв'язку більша у разі адсорбції іона металу на поверхні ОВНТ С<sub>48</sub>, у порівнянні з адсорбцією на фуллерені С<sub>60</sub>. Оскільки комплекси Cu<sup>2+</sup> були найбільш термодинамічно стабільними, енергія зв'язку зростала у такій послідовності Co<sup>2+</sup><Zn<sup>2+</sup><Ni<sup>2+</sup><Cu<sup>2+</sup>. Результати розрахунків вільної енергії зв'язку показали хорошу кореляцію з шириною забороненої зони, відстанями між іоном металу і поверхнею ВНЧ, дипольними моментами, делокалізацією заряду у методі природних орбіталей (МПО) і другим потенціалом іонізації іонів металів.

*Ключові слова:* електроосадження; композиційні матеріали; перехідні метали; вуглецеві наночастинки; ТФГ.

## АДСОРБЦИЯ ИОНОВ МЕТАЛЛОВ Co, Ni, Cu, Zn НА ФУЛЛЕРЕНЕ C60 И НА ОДНОСТЕННОЙ УГЛЕРОДНОЙ НАНОТРУБКЕ C48 КАК ДЕЙСТВУЮЩАЯ СИЛА ЭЛЕКТРООСАЖДЕНИЯ КОМПОЗИЦИОННЫХ ПОКРЫТИЙ

Валентина В. Титаренко<sup>1</sup>, Эдуард Ф. Штапенко<sup>1</sup>, Евгений О. Воронков<sup>1</sup>, Аруна Вангара<sup>2</sup>, Владимир А. Заблудовский<sup>1</sup>, Войцех Колоджейчик<sup>3</sup>, Карина Капуста<sup>3</sup>, Сергей И. Оковитый<sup>4</sup>  
<sup>1</sup>Днепро́вский национальный университет железнодорожного транспорта имени академика В. Лазаряна, г. Днепр, 49010, Украина

<sup>2</sup>Раст-колледж, Холли-Спрингс, штат Массачусетс, 38635, США <sup>3</sup>Междисциплинарный центр нанотоксичности, Кафедра химии, физики и атмосферных наук, Государственный университет Джексона, Джексон, штат Массачусетс, 39217, США

<sup>4</sup> Днепро́вский национальный университет им. Олеса Гончара, Днепр, 49010, Украина

### Аннотация

Исследованы композиционные пленки, осажденные из водных растворов электролитов, содержащих ионы металлов и частицы углеродных наноматериалов, таких как фуллерен С<sub>60</sub>. Результаты исследования катодных поляризационных кривых показали увеличение сопротивления переноса заряда. Анализ фазового состава металлических пленок показал наличие углеродных наночастиц (УНЧ) внутри металлической матрицы и значительные изменения в кристаллической решетке. Из результатов исследования микрофотографий следует, что добавление УНЧ изменяет структуру роста металлических пленок от столбчатой к микрослоистой из-за пассивации поверхности. В данной работе теория функционала плотности (ТФП) была использована для расчета термодинамических, электронных и структурных свойств комплексов ионов металлов с УНЧ. Результаты расчетов энергии связи комплексов УНЧ-Ме<sup>2+</sup> позволяют предположить, что адсорбция ионов Co<sup>2+</sup>, Ni<sup>2+</sup>, Cu<sup>2+</sup> и Zn<sup>2+</sup> на поверхности фуллерена С<sub>60</sub> и одностенной углеродной нанотрубки (ОУНТ) С<sub>48</sub> возможна и термодинамически выгодна. Было обнаружено, что энергия связи больше в случае адсорбции иона металла на поверхности ОУНТ С<sub>48</sub>, в сравнении с адсорбцией на фуллерене С<sub>60</sub>. Поскольку комплексы Cu<sup>2+</sup> были наиболее термодинамически стабильными, энергия связи возрастала в такой последовательности Co<sup>2+</sup> < Zn<sup>2+</sup> < Ni<sup>2+</sup> < Cu<sup>2+</sup>. Результаты расчетов свободной энергии связи показали хорошую корреляцию с шириной запрещенной зоны, расстояниями между ионом металла и поверхностью УНЧ, дипольными моментами, делокализацией заряда в методе естественных орбиталей (МЕО) и вторым потенциалом ионизации ионов металлов.

*Ключевые слова:* электроосаждение; композиционные материалы; переходные металлы; углеродные наночастицы; ТФП.

### Introduction

Currently, carbon nanoparticles are widely used in material science as fillers for composite materials [1; 2]. When CNPs are doped into a metal matrix, it increases the hardness, durability and corrosion resistance of a material [3–8]. These unique properties are enhancing an interest in development CNPs doped metallic composites. However, the high costs of their production lead scientists to investigate the materials hardened only on the surface by covering it with metallic films doped with CNPs. One widely used approach for production of CNPs-metal films is a method that utilizes steam condensation onto a substrate surface [9; 10]. Another method is based on electrodeposition of composite films from the aqueous solution which contains both metal ions and CNPs (co-deposition). This method allows one to control the nucleation and growth of a composite CNPs-metal film by applying different impulse current, ultrasound, magnetic field, and external laser radiation. The unique

physicochemical properties of electrodeposited films largely depend on the concentration of CNPs in the metal matrix. Therefore, controlling the CNPs' content in composite metal films is crucial for researchers. Despite that, the mechanism of co-deposition of such films remains not fully understood. A number of works suggested that the transfer of CNPs to electrode surface occurs exclusively by the convection flow, which is created by metal ions in the electrolyte solution [11; 12]. The other works [13; 14] proposed the idea that the CNPs' are charging in the electrolyte solution and move towards cathode under the influence of an electric field created by the difference in potential between the anode and the cathode.

Computational chemistry has a great potential in the prediction and clarification of mechanisms that are not proved experimentally [15]. Density functional theory (DFT) has recently taken a place as one of the most popular methods for calculating the electronic structure of atoms, molecules,

clusters, solids, etc. [16; 17]. Popularity of DFT grows, primarily, due to the combination of a sufficient accuracy and very moderate requirements for computational resources. Relatively low computational time allows to calculate systems consisting of hundreds of atoms that is necessary for a modern nanotechnology [18]. Numerous studies devoted to characterization of molecules and clusters using the DFT [19] have shown good results when correct exchange-correlation functional has been chosen. As noted in [20; 21], one of the most suitable for calculating the structural and thermochemical characteristics of metal complexes is the three-parameter hybrid functional B3LYP [22]. The density functional theory using hybrid functionals makes it possible to successfully calculate the structural and electronic characteristics of transition and heavy metals with acceptable computer time [23].

The possibility of metal atoms to be adsorbed on CNPs' surface has been previously studied using DFT methods [24; 25]. There have been a small number of investigations regarding a mechanism of electrodeposition of CNPs doped metal films. Valencia et al. [25] calculated the binding energies between transition metals and CNPs such as fullerene  $C_{60}$  and SWNTs  $C_{48}$  using DFT in order to explain the mechanism of metal atoms' adsorption on the surface of CNPs in gas phase. It was shown that the value of the binding energy between CNPs and a metal adsorbed on its surface varied in the range of  $0.05 \pm 2$  eV, depending on the metal. Simulations were carried out for adsorption of neutral atoms on a neutral surface in vacuum.

In this work, an experimental study has been combined with computational techniques aiming the goal of characterization of electrodeposited complexes and clarification of hypothesis proposed here as for electrodeposition mechanism. The phase composition analysis of electrodeposited composite metal films has been carried out as well as the cathode polarization curves of an aqueous nickel and zinc plating electrolyte solution with fullerene  $C_{60}$  NPs have been reported. 3D structures of metal carbon nanoparticle complexes have been proposed. Quantum-chemical calculation have been carried out for determination of complexes' formation thermodynamical properties (binding energies, entropies, and free Gibb's energies) for  $C_{48}+Me^{2+}$  (Co, Ni, Cu, Zn) and  $C_{60}+Me^{2+}$  (Co, Ni, Cu, Zn).

## Theory and Methodology

*Experiment methodology.* Composite metal films have been precipitated from aqueous solutions of electrolytes of the following compositions (in g/l):  $Ni_2SO_4 \cdot 7H_2O$  – 300,  $H_3BO_3$  – 30,  $Na_2SO_4 \cdot 10H_2O$  – 50,  $C_{60}$  – 0.5 (pH 5.0);  $ZnSO_4 \cdot 7H_2O$  – 250,  $Na_2SO_4$  – 75,  $Al_2(SO_4)_3$  – 30,  $C_{60}$  – 0.5 (pH 4.0). Pure nickel (zinc) plate was used as anode, which made it possible to maintain the concentration of main metal salt unchanged and had a positive impact on the repeatability of experiments. The electrodes were placed parallel to each other in order to provide the uniformity of the electric field. CNPs were kept suspended in the volume of an electrolyte solution using magnetic stirring to prevent the particles from conglomerating on the bottom of the electrolytic cell. Electrodeposition of composite CNPs films of nickel and zinc was carried out in a galvanostatic mode at applied current density value  $100 A/m^2$ . The same electrodeposition mode was used to fabricate metal films from aqueous electrolyte solutions that did not contain CNPs.

Potentiodynamic polarization experiments have been performed using a P-5827M Potentiostat at the scan rate of 10 mV/s. All the measurements have been carried out in a three-electrode electrolytic cell. A copper plate has been used as the working electrode (cathode). A silver chloride electrode has served as a reference electrode, and a platinum electrode has been used as an auxiliary electrode.

X-ray phase analysis of the films obtained with the same electrolysis conditions have performed on a DRON-2.0 Diffractometer using scintillation counter for X-ray detection. Phase composition determination of the films was carried out in monochromatic Co-K $\alpha$  radiation.

The microstructure of the films in the cross-section was investigated using an optical microscope "Neophot-21". Microsections for metallographic studies were mechanically polished and chemically cured in a 50% solution of nitric acid for 10-15 s.

*Computational details.* Some model approximations have been considered for calculation of the binding energy of metal ions with CNPs:

I. Adsorption occurs in electrolyte solutions, in particular in aqueous solutions, which requires the choice of a solvent model. Polarizable Continuum Model (CPCM) [26] with water has been used as a solvation model.

II. Complexes formed by adsorption of metal ions on surface of CNPs must have a charge equivalent to a total charge of all ions absorbed.

III. Adsorption of metal ions on a surface of CNPs occurs alternately. Each subsequent metal ion is adsorbed on a CNP, which already has a charge obtained by the previous adsorption.

Calculations of the binding energies for transition metals were carried out using the B3LYP functional. The choice of the basis set was based on the fact that the calculation of energy and thermodynamic quantities had been performed for metals, for which the interaction of valence electrons plays the most important role. Three basis sets were used for a comparison, including 6-31G, extended 6-31-G(d), and 6-31-G(d,p). For proper geometry optimization of the complexes, we have also taken into account the dispersion corrections [27; 28]. All calculations were carried out using the GAUSSIAN 09 program package [29].

Prior actual calculations optimization was performed for compounds with different multiplicities in order to verify which ground state is more favorable. For complexes with an even number of electrons (zinc and nickel containing complexes) multiplicities 1, 3, and 5 were used, while for the ones containing an odd number of electrons (copper and cobalt complexes) structures with multiplicities 2, 4, and 6 were tested. The results of this test revealed that the ground state of zinc is a singlet, and copper's ground state is a duplet. Higher multiplicities are typical for complexes of cobalt and nickel, having a quadruplet and triplet as a ground state, which can be explained by their ferromagnetic properties. Thus, all further calculations were carried out with multiplicities 1, 2, 3, and 4 for Zn, Cu, Ni, and Co, respectively.

The binding energies ( $\Delta W$ ) between the adsorbed metal ion and CNP were calculated as the difference between the total energy of the complex with the adsorbed metal ion ( $TE_{\text{CNP-Me}^{2+}}$ ) and the sum of the energies of its constituent parts ( $TE_{\text{CNP}}, TE_{\text{Me}^{2+}}$ ):

$$\Delta W = TE_{\text{CNP-Me}^{2+}} - (TE_{\text{CNP}} + TE_{\text{Me}^{2+}})$$

Same principle was used for calculation of enthalpies, entropies, and Gibbs free energies.

Gaussian NBO Version 3.1 was used for calculation of Natural Bond Orbitals. HOMO and LUMO orbitals and molecular electrostatic potential surfaces were visualized using GaussView6 program package.

## Results and discussion

*Experimental part.* Composite CNPs-metal films have been deposited from aqueous solutions and subjected to further investigation. XRD pattern of composites CNPs-metal films based on nickel is illustrated on Figure 1a. For comparison diffraction pattern of the fullerene  $C_{60}$  powder without impurities and the one of pure nickel is illustrated on Figures 1b and 1c, respectively. Both XRD patterns of  $C_{60}$ -Ni composite film and pure nickel have five characteristic peaks 2.03Ni, 1.26Ni, 1.24Ni, 1.06Ni, and 1.01Ni, that are corresponding to Miller indices (111), (200), (220), (311), (222), respectively. However, intensities of these peaks are varying significantly. In case of pure nickel (Figure 1c) intensity distribution is close to reference one. Maxima intensity corresponds to (111) reflection, that follows Bravais rule [30]. Meanwhile, XRD pattern of  $C_{60}$ -Ni composite film (Figure 1a) has the highest intensity peak corresponding to (220) reflection. CNPs, presumably, are blocking the active surface of the film preventing the further growth and giving the way for new centers of nucleation to appear. Faces that are parallel to internal planes with the minimal speed of growth (111) are the most prominent in case of equilibrium crystallization, while during a nucleation process the most common directions are the ones with high indices. That explains redistribution of XRD peaks' intensities.

Shifts on cathodic polarization curves might give a better understanding on a charge transfer mechanism. As it is seen from obtained cathodic polarization curves in an aqueous nickel plating (Figure 3-a) and zinc plating electrolyte (Figure 3-b) solution, the addition of CNPs causes a shift of the cathode potential to the electronegative region, which indicates an increase in charge transfer resistance. Charge transfer resistance, presumably, changes due to the change of particles' speed. Complexes of metal-CNPs are significantly larger in size than free cations, which cause their speed to be lower, compare to ones in the solution without CNPs. This observation supports the idea about the formation of metal-CNPs complexes in the solution with further movement towards cathode, which explains the formation of an axial growth pattern with large crystallographic indices (Figure 1-a).

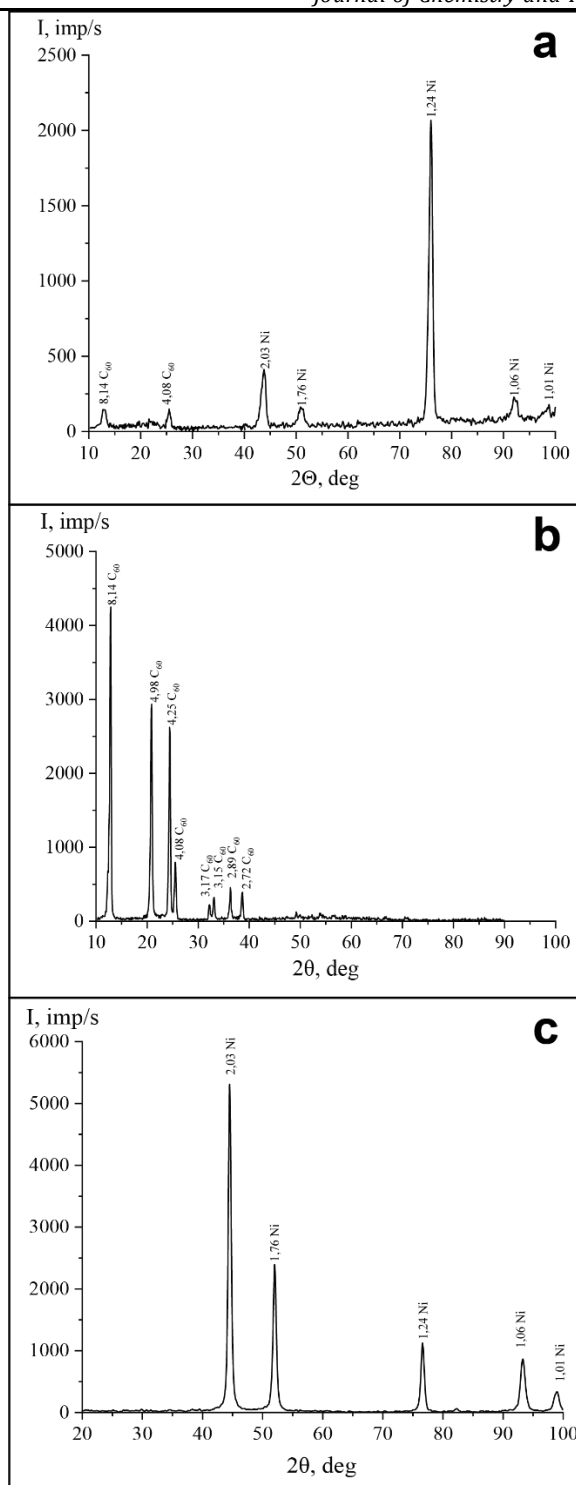


Fig. 1. XRD pattern of a - Ni-C<sub>60</sub> composite film; b - fullerene C<sub>60</sub>; c - and nickel.

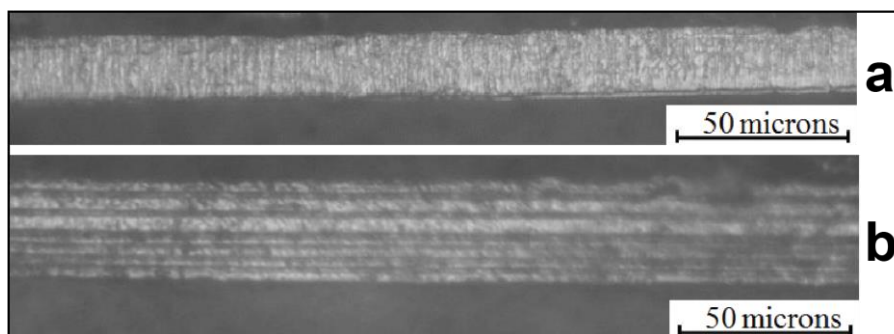


Fig. 3. Microphotography of nickel (a) and Ni-C<sub>60</sub> composite (b) films in cross section.

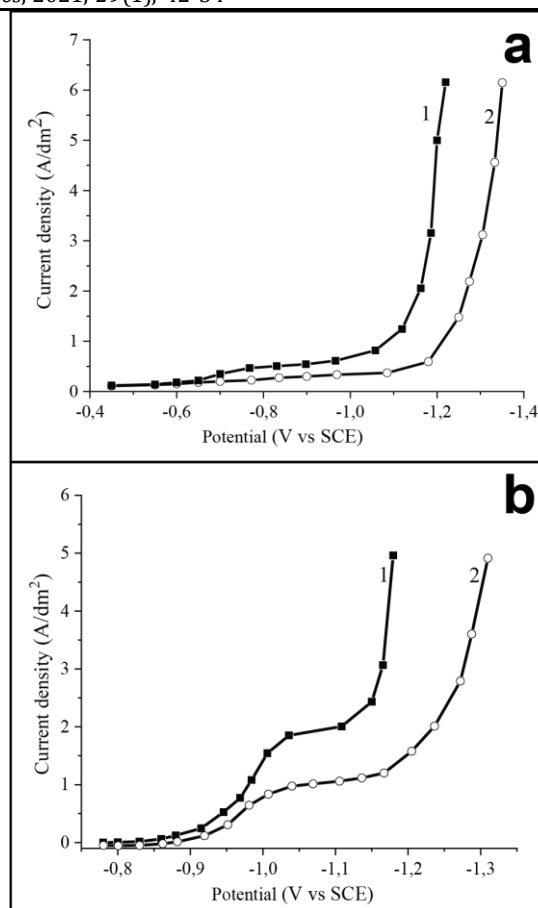


Fig. 2. Cathodic polarization curves obtained in a - hydrosulfate nickel plating electrolyte and b - zinc plating electrolyte: 1 - without CNPs; 2 - with presence of CNPs.

Layered structure of a composite film can be explained by formation of a passive layer on a surface of cathode. In case when the energy of charged CNP-metal complexes is not sufficient to cross the passive layer, the formation of new nucleation centers is becoming more favorable. Nucleation centers are growing due to further adsorption of complexes on it. Consequently, a layered structure is formed by a Mechanisms of Stranski-Krastanov growth [31].

Experimental characterization tells us about presence of numerous nucleation centers, due to disturbance of surface by CNPs, however, it cannot give a description of how CNPs are delivered to the surface section.

*Structures of CNP-Me<sup>2+</sup> complexes and their thermodynamic properties.* In order to prove the hypothesis proposed here complexes of fullerene C<sub>60</sub> and carbon nanotube SWNT C<sub>48</sub> with Ni<sup>2+</sup>, Co<sup>2+</sup>, Cu<sup>2+</sup>, and Zn<sup>2+</sup> were optimized in aqueous solution (Fig. 4). Minimum energy structures of C<sub>60</sub>-metal complexes in case of cobalt, zinc and nickel ions had ion located above one of the carbon atoms. While position of ion above the middle of a C-C bond connecting C<sub>6</sub> and C<sub>5</sub> rings was the most energetically favorable for C<sub>60</sub>-Cu<sup>2+</sup> complex. More complicated results were obtained for C<sub>48</sub>-metal complexes. In this case Ni<sup>2+</sup> was located above the middle of a C-C bond, Zn<sup>2+</sup> showed to be more favorable in the middle of C<sub>6</sub> cell, while Co<sup>2+</sup> and Cu<sup>2+</sup> position was above the C<sub>6</sub> cell shifted towards one of the bonds. Calculations using all three basis sets showed the same positions of the metal ions on a surface of SWNT C<sub>48</sub>, but for fullerene C<sub>60</sub> results obtained by 6-31G basis set were

significantly different from the ones obtained by more extended basis sets.

Optimized distances between transition metal ions and CNPs' surface are significantly smaller in case of SWNT C<sub>48</sub> (Fig. 4) with the trend of increasing optimized distance in a row Cu<Co<Zn<Ni. Meanwhile for fullerene this trend is different increasing in a row Cu<Zn<Ni<Co. As for dipole moment in most cases its vector is perpendicular to the surface of CNPs and directed through the metal ion, except for C<sub>48</sub>-Co<sup>2+</sup> and C<sub>48</sub>-Ni<sup>2+</sup>. Position of Ni<sup>2+</sup> above the C-C bond directs dipole moment from the middle of nanotube towards one of nanotube's sides, and consequently causing localization of a charge, making an opposite side being more negative. Even though complex C<sub>48</sub>-Co<sup>2+</sup> visually look more similar to the one of C<sub>48</sub> with Cu<sup>2+</sup>, it's insignificantly shifted towards one of the sides (with deviation 0.1 Å), which leads to a similar charge distribution as in case of C<sub>48</sub>-Ni<sup>2+</sup>.

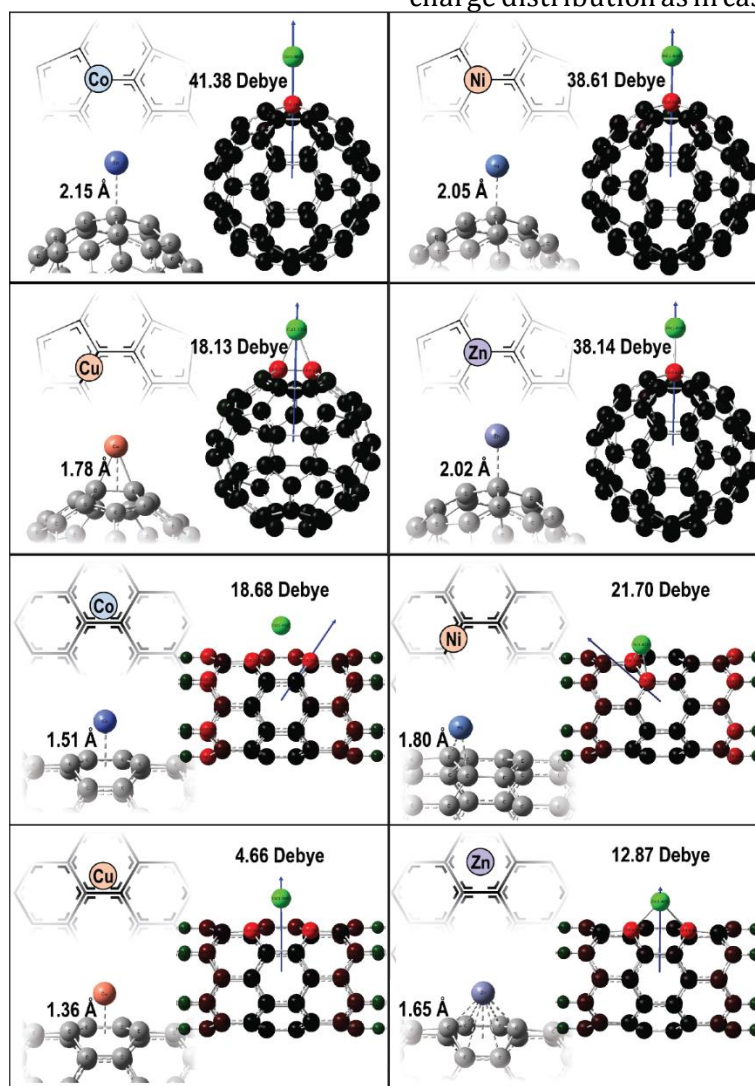


Fig. 4. Location of metal ion adsorbed on a surface of fullerene C<sub>60</sub> and SWNT C<sub>48</sub>, the distance and the direction of a dipole moment vector.

Thermodynamic parameters calculated using three different basis sets are collected in Table 1. It can be seen that all of the metal ions are strongly bound to C<sub>48</sub> and C<sub>60</sub>, since their binding energies ( $\Delta W$ ) exceeds the thermal movement energy of 0.025 eV (0.58 kcal/mol). Results vary slightly for minimal 6-31G basis set especially for C<sub>60</sub> complexes. This fact suggests that minimal basis set may not be enough accurate for description of transition metal adsorption, since two d-orbitals are not enough for a proper description of partially filled d-orbital of these metal ions. Binding energies calculated using extended 6-31G(d,p) showed to decrease in a row Co>Zn>Ni>Cu and C<sub>60</sub>>C<sub>48</sub>. Interestingly binding energies of copper containing complexes are at least twice larger by module than the ones of CNPs complexes with nickel and other metals.

Since theoretically there is a possibility that more than one metal ion is adsorbed on a surface of CNPs, we have taken into consideration models with one fullerene C<sub>60</sub> bound to up to six metal ions. According to approximation II from *Computational details* section, with addition of each new metal ion the charge of the system should increase on 2e. Models of complexes with 1, 2, 3, 4, and 5 bound metal ions that have charges +2e, +4e, +6e, +8e, and +10 e, respectively, were proposed and optimized (Fig. 5). With the sequential addition of metal ions to C<sub>60</sub>, binding energies showed to decrease. One can see that addition of a second Co<sup>2+</sup> and a second Ni<sup>2+</sup> ion resulted in thermodynamically unstable structure with 64.34 kcal/mol and 3.80 kcal/mol Gibbs free energy, respectively. Addition of a second Zn<sup>2+</sup>,

and Cu<sup>2+</sup>, meanwhile, yielded negative Gibbs free energy values, despite the fact that they are significantly higher compare to free energies of first metal ion adsorption. Systems with total charge +6e due to adsorption of a third metal ion were stable for Cu<sup>2+</sup> and showed to be unfavorable for Zn<sup>2+</sup> complex. In case of copper up to 5 ions can be adsorbed on a surface of fullerene, with total charge +10e, while addition of the sixth ion is thermodynamically unfavorable. Considering extremely high affinity of copper ion to fullerene nanoparticle, a model containing two fullerenes and one Cu<sup>2+</sup> ion was simulated and resulted in a stable complex with -24.48 kcal/mol Gibbs free energy. Addition of the third fullerene nanoparticle would make no sense, due to steric clashes between nanoparticles.

To justify the difference in binding affinity an investigation of an electronic structure was performed. Molecular electrostatic potential surfaces (MEPS) illustrated on Fig. 6 revealed that, contrary to all the other CNP-Me<sup>2+</sup> complexes, complexes of copper characterized with a strong delocalization of electron density, thus stabilizing whole complex. Calculation of Natural Bond Orbital (NBO) confirmed this observation, showing that +2 positive charge was compensated, yielding partial charges on CNPs +0.93 and +0.77 and partial charges on copper +1.07 and +1.23 for complex with C<sub>48</sub> and C<sub>60</sub>, respectively, (Table 3). Other metal ions similarly to Cu showed strong acceptor properties, though, delocalization in this case was not that strong.

Table 1

| Complex | $\Delta W$ , kcal/mol |          |            | $\Delta H$ , kcal/mol |          |            | $\Delta S$ , cal/mol K |          |            | $\Delta G$ , kcal/mol |          |            |
|---------|-----------------------|----------|------------|-----------------------|----------|------------|------------------------|----------|------------|-----------------------|----------|------------|
|         | 6-31G                 | 6-31G(d) | 6-31G(d,p) | 6-31G                 | 6-31G(d) | 6-31G(d,p) | 6-31G                  | 6-31G(d) | 6-31G(d,p) | 6-31G                 | 6-31G(d) | 6-31G(d,p) |
| C48+Co  | -44.13                | -47.73   | -50.11     | -42.82                | -46.10   | -48.59     | -27.44                 | -26.27   | -27.62     | -34.64                | -38.27   | -40.35     |
| C48+Ni  | -69.95                | -74.78   | -74.86     | -68.77                | -73.37   | -73.47     | -28.40                 | -29.24   | -29.71     | -60.30                | -64.65   | -64.62     |
| C48+Cu  | -155.14               | -166.48  | -166.51    | -153.62               | -163.90  | -163.95    | -25.27                 | -31.08   | -31.30     | -146.08               | -154.63  | -154.61    |
| C48+Zn  | -56.80                | -63.14   | -63.17     | -54.50                | -60.35   | -60.42     | -29.36                 | -31.31   | -31.28     | -45.74                | -51.02   | -51.10     |
| C60+Co  | -56.75                | -9.26    | -8.93      | -57.00                | -8.94    | -8.67      | -30.26                 | -28.11   | -27.31     | -47.98                | -0.56    | -0.52      |
| C60+Ni  | -73.89                | -8.33    | -27.16     | -74.11                | -8.28    | -26.82     | -30.94                 | -25.74   | -28.70     | -64.88                | -0.61    | -18.26     |
| C60+Cu  | -133.38               | -86.90   | -98.42     | -134.98               | -86.24   | -98.99     | -27.19                 | -27.28   | -27.79     | -126.87               | -78.11   | -90.71     |
| C60+Zn  | -66.05                | -19.97   | -19.97     | -66.23                | -19.46   | -19.49     | -28.67                 | -26.63   | -26.62     | -57.68                | -11.52   | -11.55     |

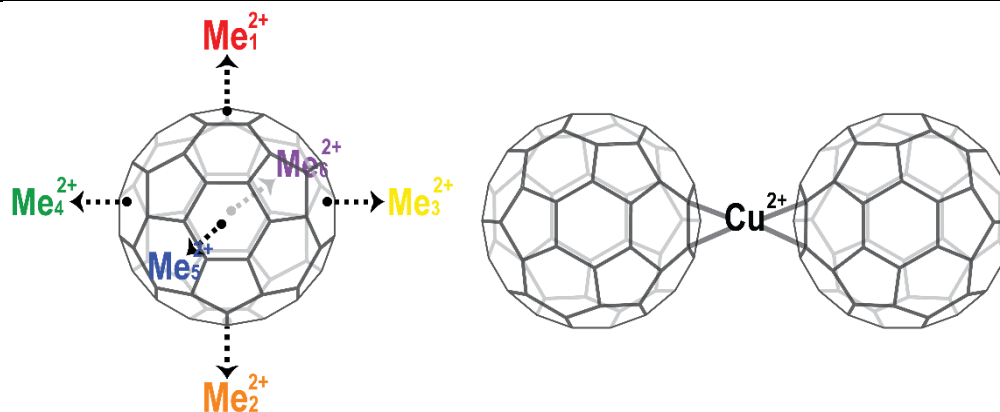


Fig. 5. Models of: a - one carbon nanoparticles and several metal ions, and b - two carbon nanoparticles and one metal ion.

Table 2

| Stability of complexes containing one fullerene nanoparticle and several metal ions. |              |        |        |        |        |     |
|--|--------------|--------|--------|--------|--------|-----|
| Complex of C <sub>60</sub> with  | ΔG, kcal/mol |        |        |        |        |     |
|  | 2e           | 4e     | 6e     | 8e     | 10e    | 12e |
| Co   | -0.52        | >0     | >0     | >0     | >0     | >0  |
| Ni   | -18.26       | >0     | >0     | >0     | >0     | >0  |
| Cu   | -90.71       | -67.57 | -53.29 | -30.56 | -10.97 | >0  |
| Zn   | -11.55       | -5.57  | >0     | >0     | >0     | >0  |

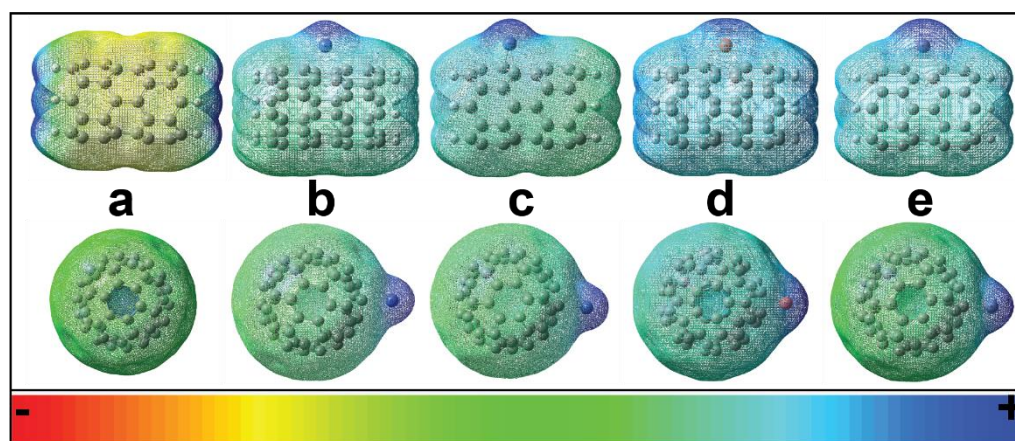


Fig. 6. Molecular electrostatic potential surfaces. a - CNP; b - CNP-Co<sup>2+</sup>; c - CNP-Ni<sup>2+</sup>; d - CNP-Cu<sup>2+</sup>; e - CNP-Zn<sup>2+</sup>.

When looking into a HOMO-LUMO gap, one must take into account that only CNP-Zn<sup>2+</sup> is a singlet, while in case of other complexes introduced with higher multiplicities, both spin-up ( $\alpha$ ) and spin-down ( $\beta$ ) should be considered. In case of the open-shell model (unrestricted DFT) the term HOMO-LUMO gap is not applicable anymore. Instead, one can look at two different excitations: from singly occupied molecular orbital to lowest unoccupied one (SOMO-LUMO transition) characteristic for  $\beta$ -spin, and HOMO-SOMO transition or d-d transition, characteristic for  $\beta$ -spin. One can notice that the  $\alpha$  gap values are significantly smaller in case of metal ions

adsorbed on a surface of C<sub>48</sub> (Fig. 7), compare to ones calculated for C<sub>60</sub> complexes (Fig. 8). HOMO(SOMO)-LUMO gap appeared to be the smallest for Cu<sup>2+</sup> complexes with 0.0025 eV for C<sub>48</sub>-Cu<sup>2+</sup> and 3.26 eV for C<sub>60</sub>-Cu<sup>2+</sup>. As expected, with an increase of gap values the complexes are becoming less stable. The only exception was observed for fullerene complexes, where band gap of fullerene bound with Ni<sup>2+</sup> is larger than the one of Zn<sup>2+</sup>, The same orbitals are participating in this transition for both complexes C<sub>60</sub>-Ni<sup>2+</sup> and C<sub>60</sub>-Co<sup>2+</sup>, that results their band gaps being similar in energy.

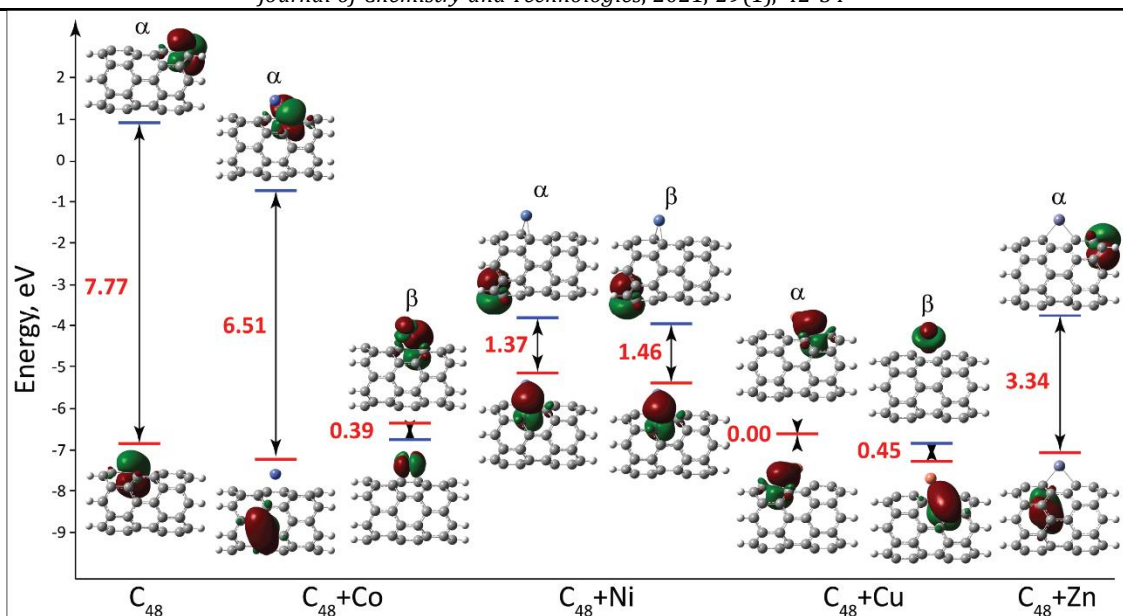


Fig. 7. Visualization HOMO (SOMO) and LUMO for metal complexes with SWNT  $C_{48}$  and band gap values.  $\alpha$ -stands for spin-up (SOMO-LUMO), and  $\beta$ -stands for spin-down (d-d transition).

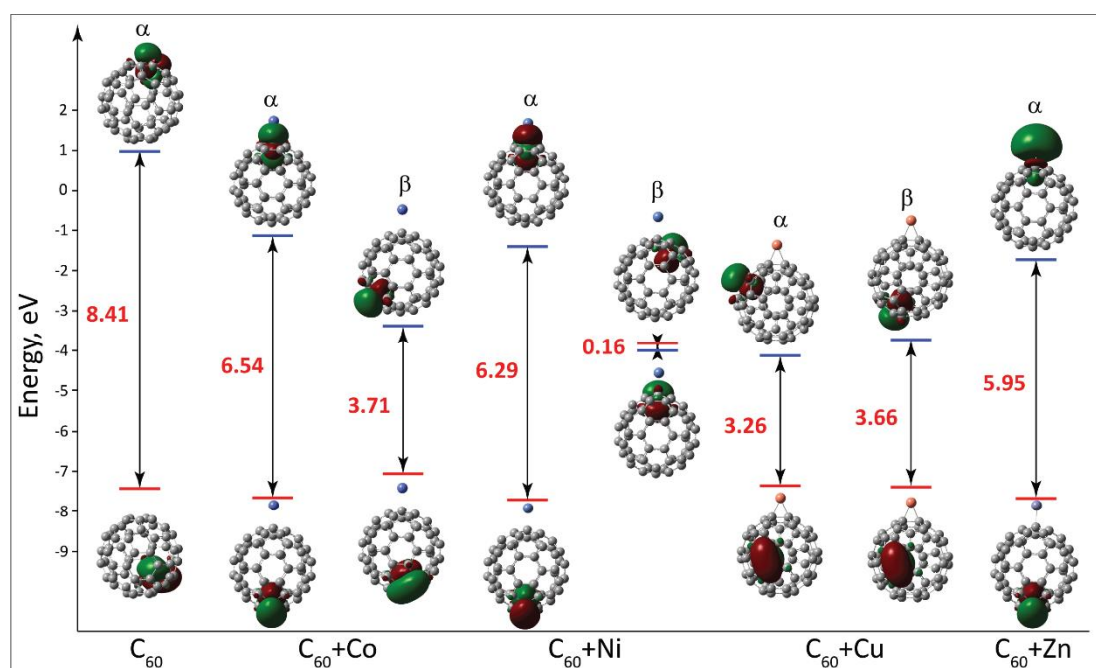


Fig. 8. Visualization HOMO (SOMO) and LUMO for metal complexes with fullerene  $C_{60}$  and band gap values.  $\alpha$ -stands for spin-up (SOMO-LUMO), and  $\beta$ -stands for spin-down (HOMO-SOMO transition)

Interestingly, copper is the only one metal ion, orbitals of which do not participate in excitation of a fullerene complex. As for the  $\beta$  spin excitations only in case of  $C_{48}$ - $Co^{2+}$  complex d-d transition occurred. Other excitations include transitions from d-orbitals of a metal ion onto the other part of a complex and *vice versa*, or do not include d-orbitals at all ( $C_{60}$ - $Cu^{2+}$ ).

Not only the band gaps but also other parameters including a distance between metal ion and a surface of CNP ( $r$ ), dipole moment ( $d$ ) and natural bond orbital (NBO) charge ( $q$ ) have a

good correlation with free Gibb's energies (Table 3). Binding affinity showed to increase with a decrease of distance between ion and a surface of a nanoparticle, which provides a better overlap of orbitals. Higher binding affinities also characterized by better delocalization of electron density with metal ion being an acceptor and conjugated  $\pi$ -system of nanoparticle being a donor of electrons. Interestingly a good agreement was observed between free binding energies and a second ionization potential of metal (Fig. 9).

| Other properties |        |          |            |           |                         |
|------------------|--------|----------|------------|-----------|-------------------------|
| Complex          | r, Å   | d, Debye | q (CNP), e | q (Me), e | HOMO(SOMO)-LUMO gap, eV |
| C48+Co           | 1.51   | 18.68    | 0.52       | 1.48      | 6.51                    |
| C48+Ni           | 1.8    | 21.7     | 0.60       | 1.40      | 1.37                    |
| C48+Cu           | 1.36   | 4.66     | 0.93       | 1.07      | 0.00                    |
| C48+Zn           | 1.65   | 12.87    | 0.51       | 1.49      | 3.34                    |
| C60+Co           | 2.15   | 41.38    | 0.11       | 1.89      | 6.54                    |
| C60+Ni           | 2.05   | 38.61    | 0.16       | 1.84      | 6.29                    |
| C60+Cu           | 1.78   | 18.13    | 0.77       | 1.23      | 3.26                    |
| C60+Zn           | 2.02   | 38.14    | 0.15       | 1.85      | 5.95                    |
| R                | 0.8075 | 0.8757   | -0.9486    | 0.9486    | 0.8803                  |

Overall high values of binding energies between metal ions and CNPs supports the idea of cations being adsorbed on the surface of CNPs before all complexes can move to cathode.

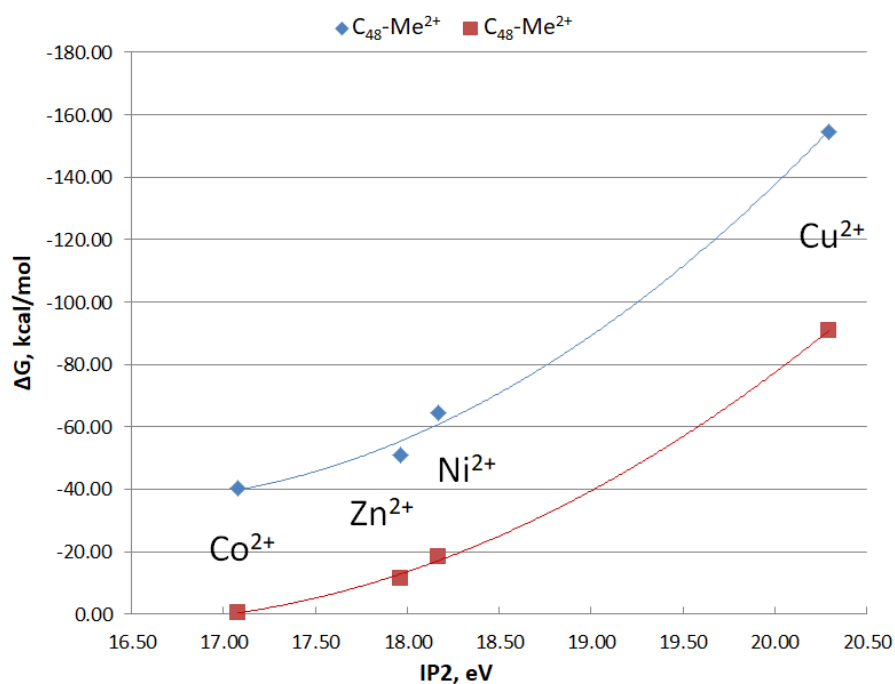


Fig. 9. Dependence of binding free energy ( $\Delta G$ ) on a second ionization potential ( $IP_2$ ).

## Conclusions

Composite electrodeposited films were fabricated and characterized. Results of characterization have shown the increase in charge transfer resistance due to change of particles' speed. Presumably, it can be caused by an increase of particle mass. Microphotographies of a C<sub>60</sub>-Ni<sup>2+</sup> composite film showed a layered pattern of deposition. If the transfer would occur exclusively by the convection flow, like it was suggested before, structure of a deposit would be more disordered. Thus, here we proposed a mechanism of metal ions being adsorbed on a surface of CNPs with further movement of the charged complex towards cathode.

Stated hypothesis was tested computationally. Comparison of calculated binding energies of the CNP-Me<sup>2+</sup> complexes with the energies of thermal motion has showed that in an aqueous solution,

adsorption of Co<sup>2+</sup>, Ni<sup>2+</sup>, Cu<sup>2+</sup>, and Zn<sup>2+</sup> ions on the surface of fullerene C<sub>60</sub> and SWNT C<sub>48</sub> is possible and thermodynamically favorable with the formation of stable composite carbon-metal complexes. Binding affinity showed to be much stronger in case of an adsorption on a surface of SWNT C<sub>48</sub>, compare to fullerene C<sub>60</sub>, and increase in row Co<sup>2+</sup><Zn<sup>2+</sup><Ni<sup>2+</sup><Cu<sup>2+</sup>. Clear dependences between free binding energy and different parameters, such as a band gap, a distance between metal ion and a surface of CNPs, dipole moment, delocalization of natural bond orbital (NBO) charge, and second ionization potential of a metal were observed. Both experimental and computational studies support proposed here hypothesis regarding a mechanism of CNPs co-deposition.

## Compliance with ethical standards

The authors declare that they have no known

competing financial interests or personal relationships that could have appeared to influence the work reported in this paper.

### Funding information

The authors want to thank the National Science Foundation [Grant: NSF/CREST HRD-1547754] for financial support.

### Bibliography

- [1] He X. Wang Y. Preparation and Investigation of Ni-Diamond Composite Coatings by Electrodeposition / He X. Y. Wang, X. Sun, L. Huang // *Nanosci Nanotechnol Lett.* – 2012. – № 4. – С. 48–52.
- [2] Preparation of composite electrochemical nickel-diamond and iron-diamond coatings in the presence of detonation synthesis nanodiamonds / G.K. Burkat, T. Fujimura, V.Y. Dolmatov, E.A. Orlova // *Diam Relat Mater.* – 2005. – V.14 (11). – P.1761–1764.
- [3] Structure and properties of chromium-nanodiamond composite electrochemical coatings / V.P. Isakov, A.I. Lyamkin, D.N. Nikitin [et al.] // *Prot Met Phys Chem Surfaces.* – 2010. V. 46. – P.78–581.
- [4] Effects of nano-diamond particles on the structure and tribological property of Ni-matrix nanocomposite coatings / L.Wang, Y. Gao, Q. Xue [et al.] // *Mater Sci Eng.* – 2005. – A 390 (1-2). – P. 313–318.
- [5] Zabludovsky V.A. The investigation of influence of laser radiation on the structure and mechanical properties of composite electrolytic nickel coating / V.A. Zabludovsky, V.V. Dudkina, E.F. Shtapenko // *Science and Transport Progress Bulletin of Dnipropetrovsk National University of Railway Transport.* – 2013. – №5 (47). – P. 70–78.
- [6] Dudkina V. V. The structure and properties of electrolytic nickel composite coatings fabricated by pulse current / V.V. Dudkina, V.A. Zabludovskiy, E. F. Shtapenko // *Metallofiz I Noveishie Tekhnologii.* – 2015. – V. 37., №5. – P. 713–72.
- [7] Tytarenko V.V. The effect of superdispersed diamond particles on the structure and properties of electrolytic nickel coatings / V.V. Tytarenko, V.A. Zabludovskyy // *Metallofiz I Noveishie Tekhnologii.* – 2016. – V. 38. – №4. – P. 519–529.
- [8] Application of pulse current for producing a strengthening composite nickel coating / V. V. Tytarenko, V.A. Zabludovsky, E. P. Shtapenko, I.V. Tytarenko // *Galvanoteknik.* – 2019. – V. 110. – №4. – P. 648–65.
- [9] Wanniarachchi A.S. Film condensation of steam on horizontal finned tubes: effect of fin spacing / A.S. Wanniarachchi, P.J. Marto, J.W. Rose // *J. Heat Transfer.* – 1986. – V.108, № 4. – P. 960–966.
- [10] Kim S. J. Turbulent film condensation of high pressure steam in a vertical tube / S. J. Kim, C. N. Hee // *Int. J. Heat and Mass Transfer.* – 2000. – V. 43. № 21 (1). P. 4031–4042.
- [11] Chiganova G. A. Effect of Nanodiamond Modification on the Characteristics of Diamond-Containing Nickel Coatings / G. A. Chiganova, L. E. Mordvinova // *Inorg Mater.* – 2011. – V. 47. – P. 717–721.
- [12] Co-deposition mechanism of nanodiamond with electrolessly plated nickel films / H. Matsubara, Y. Abe, Y. Chiba [et al.] // *Electrochim Acta.* – 2007. – V. 52. – № 9 (15). – P.3047–3052.
- [13] Erratum to: Synthesis and characterization of nickel-diamond nanocomposite layers / C. Gheorghies, D. E. Rusu, A. Ispas [et al.] // *Applied Nanoscience.* – 2014. – №4. – P.1021–1033.
- [14] Hou J. G. Jpcs61 / J. G. Hou, X. Li, H. Wang, B. Wang. – 2000. – 995. Pdf. – V. 61. – P. 995–998.
- [15] DFT study of the mechanism and selectivities of the [3+2] cycloaddition reaction between 3-(benzylideneamino) oxindole and trans- $\beta$ -nitrostyrene / C. Sobhi, N. A. Khorief, A. Djerourou [et al.] // *J. Physical Organic Chemistry.* – 2017. – 30:e3637.
- [16] Parr R.G. Density-Functional Theory of Atoms and Molecules. *Density Funct. Theory Atoms Mol* / R. G. Parr, W. Yang // *Horizons of Quantum Chemistry.* – 1989. – P 5–15.
- [17] Koch W. *Chemists Guide to Density Functional Theory* / W. Koch, M. C. Holthausen. – Wiley, VCH: New York, 2001.
- [18] Arbuznikov A. V. Hybrid exchange correlation functionals and potentials: Concept elaboration / A. V. Arbuznikov // *J. Struct. Chem.* – 2007. – V. 48. – № 1. – P.31.
- [19] Becke A. D. Perspective: Fifty years of density-functional theory in chemical physics / A. D. Becke // *J. Chem. Phys.* – 2014. – 140.
- [20] Schreckenbach G. Theoretical Study of Stable Trans and Cis Isomers in [UO<sub>2</sub>(OH)<sub>4</sub>] 2- Using Relativistic Density Functional Theory / G. Schreckenbach, P. J. Hay, R. L. Martin // *Inorg. Chem.* – 2002. – V. 37. – P. 4442–4451.
- [21] Schreckenbach G. Density functional calculations on actinide compounds: Survey of recent progress and application to [UO<sub>2</sub>X<sub>4</sub>] 2? (X=F, Cl, OH) and AnF<sub>6</sub> (An=U, Np, Pu) / G. Schreckenbach, P. J. Hay, R. L. Martin // *J. Comput. Chem.* – 1999. – V. 20. – P. 70–90.
- [22] Becke A. D. Density-functional thermochemistry. III. The role of exact exchange / A. D. Becke // *J. Chem. Phys.* – 1993. – V. 98. – P. 5648–5652.
- [23] Kohn W., Becke A. D., Parr R. G. Density functional theory of electronic structure / W. Kohn, A. D. Becke, R. G. Parr // *J. Phys. Chem.* – 1996. – V. 100. – P. 12974–12980.
- [24] Belenkov E. A. Structure of carbinoid nanotubes and carbinofullerenes / E. A. Belenkov, I. V. Shakhova // *Phys. Solid. State.* – 2011. – V. 53. – P. 2385–2392.
- [25] Valencia H. Trends in the adsorption of 3d transition metal atoms onto graphene and nanotube surfaces: A DFT study and molecular orbital analysis / H. Valencia, A. Gil, G. Frapper // *J. Phys. Chem.* – 2010. – V. 114. – P. 14141–14153.
- [26] A review of methods for the calculation of solution free energies and the modelling of systems in solution / R. E. Skynner, J. L. McDonagh, C. R. Groom, T. van Mourika, J. B. O. Mitchell // *Phys. Chem. Chem. Phys.* – 2015. – V.17. – P. 6174–6191.
- [27] Grimme S. A consistent and accurate ab initio parametrization of density functional dispersion correction (DFT-D) for the 94 elements H-Pu / Grimme S., Antony J., Ehrlich S., Krieg H. // *J. Chem. Phys.* – 2010. – V. 132, 154104.
- [28] Grimme S. Effect of the damping function in dispersion corrected density functional theory / S. Grimme, S. Ehrlich, L. Goerigk // *J. Comput. Chem.* – 2011. – V. 32. – P. 1456–1465.
- [29] Frisch M. J. / M. J. Frisch, G. W. Trucks, H. B. Schlegel, G. E. Scuseria, M. A. Robb, J. R. Cheeseman, G. Scalmani, V. Barone, G. A. Petersson, H. Nakatsuji, X. Li, M. Caricato, A. Marenich, J. Bloino, B. G. Janesko, R. Gomperts, B. Mennucci, H. P. Hratchian, J. V. Ortiz, A. F. Izmaylov, J. L. Sonnenberg, D. Williams-Young, F. Ding, F. Lipparini, F. Egidi, J. Goings, B. Peng, A. Petrone, T. Henderson, D.

- Ranasinghe, V. G. Zakrzewski, J. Gao, N. Rega, G. Zheng, W. Liang, M. Hada, M. Ehara, K. Toyota, R. Fukuda, J. Hasegawa, M. Ishida, T. Nakajima, Y. Honda, O. Kitao, H. Nakai, T. Vreven, K. Throssell, J. A. J. Montgomery, J. E. Peralta, F. Ogliaro, M. Bearpark, J. J. Heyd, E. Brothers, K. N. Kudin, V. N. Staroverov, T. Keith, R. Kobayashi, J. Normand, K. Raghavachari, A. Rendell, J. C. Burant, S. S. Iyengar, J. Tomasi, M. Cossi, J.M. Millam, M. Klene, C. Adamo, R. Cammi, J. W. Ochterski, R. L. Martin, K. Morokuma, O. Farkas, J. B. Foresman, D. J. Fox. – Gaussian 09, Revision D.01, 2016.
- [30] Bravais A. Études cristallographiques par M. Auguste Bravais. – Paris, Gauthier-Villars, 1866. – 283 p.
- [31] Formation of Layered Structure in Films of Nickel at Electrodeposition by a Pulse Current / E.P. Shtapenko, V.O. Zabludovsky, V.V. Tytarenko [et al.] // *Metallofizika i Noveishie Tekhnologii*. – 2019. – V.41. – №1. – P. 27–37.
- ## References
- [1] He, X. Y. Wang, X., Sun, L. (2012). Huang Preparation and Investigation of Ni-Diamond Composite Coatings by Electrodeposition. *Nanosci Nanotechnol Lett*, 4, 48–52.
- [2] Burkat, G.K., Fujimura, T., Dolmatov, V.Y., Orlova, E.A. (2005). Preparation of composite electrochemical nickel–diamond and iron–diamond coatings in the presence of detonation synthesis nanodiamonds. *Diam Relat Mater*, 14(11), 1761–1764.
- [3] Isakov, V.P., Lyamkin, A.I., Nikitin, D.N., Shalimova, A.S., Solntsev, A.V. (2010). Structure and properties of chromium-nanodiamond composite electrochemical. *Prot Met Phys Chem Surfaces*, 46, 78–581.
- [4] Wang, L., Gao, Y., Xue, Q., Qunji, X. (2005). Huiwen Effects of nano-diamond particles on the structure and tribological property of Ni-matrix nanocomposite coatings. *Mater Sci Eng. A* 390(1-2), 313–318.
- [5] Zabludovsky, V.A. Dudkina, V.V., Shtapenko E.F. (2013). The investigation of influence of laser radiation on the structure and mechanical properties of composite electrolytic nickel coating. *Science and Transport Progress Bulletin of Dnipropetrovsk National University of Railway Transport*, 5(47), 70–78.
- [6] Dudkina, V.V., Zabludovsky, V.A. Shtapenko E.F. (2015). V. The structure and properties of electrolytic nickel composite coatings fabricated by pulse current. *Metallofiz I Noveishie Tekhnologii*, 37(5), 713–72.
- [7] Tytarenko, V.V. Zabludovskyy, V.A. (2016). The effect of superdispersed diamond particles on the structure and properties of electrolytic nickel coatings. *Metallofiz I Noveishie Tekhnologii*, 38(4), 519–529.
- [8] Tytarenko, V.V., Zabludovsky, V.A., Shtapenko, E.P., Tytarenko, I.V. (2019). Application of pulse current for producing a strengthening composite nickel coating. *Galvanotechnik*, 110(4), 648–65.
- [9] Wanniarachchi, A.S., Marto, P.J., Rose, J.W. (1986). Film condensation of steam on horizontal finned tubes: effect of fin spacing. *J. Heat Transfer*, 108(4), 960–966.
- [10] Kim, S. J., Hee, C. N. (2000). Turbulent film condensation of high pressure steam in a vertical tube. *Int. J. Heat and Mass Transfer*, 43, 21(1), 4031–4042.
- [11] Chiganova, G. A., Mordvinova, L. E. (2011). Effect of Nanodiamond Modification on the Characteristics of Diamond-Containing Nickel Coatings. *Inorg Mater*, 47, 717–721.
- [12] Matsubara, H., Abe, Y., Chiba, Y., Hiroshi, N., Nobuo, S., Kazunori, H., Yasunobu, I. (2007). Co-deposition mechanism of nanodiamond with electrolessly plated nickel films. *Electrochim Acta*, 52, 9(15), 3047–3052.
- [13] Gheorghies, C. D., Rusu, E., Ispas, A., Bund, A., Carac, G., Condurache-Bota, S., Georgescu, L. P. (2014). Erratum to: Synthesis and characterization of nickel–diamond nanocomposite layers. *Applied Nanoscience*, (4), 1021–1033.
- [14] Hou, J. G., Li, X., Wang, H., Wang, B. (2000). *Jpcs*61, 995, Pdf 61, 995–998.
- [15] Sobhi, C. A., Khorief, N. A., Djerourou, A., Gutiérrez, M. R., Domingo, L. R. (2016). DFT study of the mechanism and selectivities of the [3+ 2] cycloaddition reaction between 3-(benzylideneamino) oxindole and trans- $\beta$ -nitrostyrene. *J. Physical Organic Chemistry*, 30:e3637.
- [16] Parr, R.G. Yang, W. (1989). Density-Functional Theory of Atoms and Molecules. Density Funct. Theory Atoms Mol. *Horizons of Quantum Chemistry*, 5–15.
- [17] Koch, W., Holthausen, M. C. (2001). Chemists Guide to Density Functional Theory. *Wiley, VCH: New York*.
- [18] Arbuznikov A. V. (2007). Hybrid exchange correlation functionals and potentials: Concept elaboration. *J. Struct. Chem.*, 48(1), 31.
- [19] Becke, A. D. (2014). Perspective: Fifty years of density-functional theory in chemical physics. *J. Chem. Phys.*, 140.
- [20] Schreckenbach, G. Hay, P. J., Martin, R. L. (2002). Theoretical Study of Stable Trans and Cis Isomers in [UO<sub>2</sub>(OH)<sub>4</sub>]<sup>2-</sup> Using Relativistic Density Functional Theory. *Inorg. Chem.*, 37, 4442–4451.
- [21] Schreckenbach, G., Hay, P. J., Martin, R. L. (1999). Density functional calculations on actinide compounds: Survey of recent progress and application to [UO<sub>2</sub>X<sub>4</sub>]<sup>2-</sup> (X=F, Cl, OH) and AnF<sub>6</sub> (An=U, Np, Pu). *J. Comput. Chem.*, 20, 70–90.
- [22] Becke, A. D. (1993). Density-functional thermochemistry. III. The role of exact exchange. *J. Chem. Phys.*, 98, 5648–5652.
- [23] Kohn, W., Becke, A. D., Parr, R. G. (1996). Density functional theory of electronic structure. *J. Phys. Chem.*, 100, 12974–12980.
- [24] Belenkov, E. A., Shakhova, I. V. (2011). Structure of carbinoid nanotubes and carbinofullerenes. *Phys. Solid. State*, 53, 2385–2392.
- [25] Valencia, H., Gil, A., Frapper, G. (2010). Trends in the adsorption of 3d transition metal atoms onto graphene and nanotube surfaces: A DFT study and molecular orbital analysis. *J. Phys. Chem.*, 114, 14141–14153.
- [26] Skyner, R. E., McDonagh, J. L., Groom, C. R., van Mourika, T., Mitchell, J. B. O. (2015). A review of methods for the calculation of solution free energies and the modelling of systems in solution. *Phys. Chem. Chem. Phys.*, 17, 6174–6191.
- [27] Grimme, S., Antony, J., Ehrlich, S., Krieg, H. (2010). A consistent and accurate ab initio parametrization of density functional dispersion correction (DFT-D) for the 94 elements H–Pu. *J Chem Phys*, 132, 154104.
- [28] Grimme S., Ehrlich, S., Goerigk, L. (2011). Effect of the damping function in dispersion corrected density functional theory. *J. Comput. Chem.*, 32, 1456–1465.
- [29] Frisch M. J. / M. J. Frisch, G. W. Trucks, H. B. Schlegel, G. E. Scuseria, M. A. Robb, J. R. Cheeseman, G. Scalmani, V. Barone, G. A. Petersson, H. Nakatsuji, X. Li, M. Caricato, A. Marenich, J. Bloino, B. G. Janesko, R. Gomperts, B. Mennucci, H. P. Hratchian, J. V. Ortiz, A. F. Izmaylov, J. L. Sonnenberg, D. Williams-Young, F. Ding, F. Lipparini, F. Egidi, J. Goings, B. Peng, A. Petrone, T. Henderson, D. Ranasinghe, V. G. Zakrzewski, J. Gao, N. Rega, G. Zheng, W. Liang, M. Hada, M. Ehara, K. Toyota, R. Fukuda, J. Hasegawa, M. Ishida, T. Nakajima, Y. Honda, O. Kitao, H. Nakai, T. Vreven, K. Throssell, J. A. J. Montgomery, J. E.

- Peralta, F. Ogliaro, M. Bearpark, J. J. Heyd, E. Brothers, K. N. Kudin, V. N. Staroverov, T. Keith, R. Kobayashi, J. Normand, K. Raghavachari, A. Rendell, J. C. Burant, S. S. Iyengar, J. Tomasi, M. Cossi, J.M. Millam, M. Klene, C. Adamo, R. Cammi, J. W. Ochterski, R. L. Martin, K. Morokuma, O. Farkas, J. B. Foresman, D. J. Fox. –Gaussian 09, Revision D.01, 2016.
- [30] Bravais, A. Études cristallographiques par M. Auguste Bravais. *Paris, Gauthier-Villars, 1866.*
- [31] Shtapenko, E.P., Zabludovsky, V.O., Tytarenko, V.V., Kraeva, V.S., Afanasov, A.M. (2019). Formation of Layered Structure in Films of Nickel at Electrodeposition by a Pulse Current. *Metallofizika i Noveishie Tekhnologii, 41(1), 27–37.*